TFEB SUMOylation in macrophages accelerates atherosclerosis by promoting the formation of foam cells through inhibiting lysosomal activity

Kezhou Wang
Xinhua Hospital Affiliated to Shanghai Jiaotong University School of Medicine: Shanghai Jiaotong University School of Medicine Xinhua Hospital

Wei Zhou
Shanghai Jiao Tong University School of Medicine Affiliated Renji Hospital

Gaolei Hu
Shanghai Jiaotong University: Shanghai Jiao Tong University

Lifeng Wang
Shanghai Jiaotong University School of Medicine Xinhua Hospital

Rong Cai
Shanghai Jiaotong University: Shanghai Jiao Tong University

Tian Tian (tiantianoph@163.com)
Xinhua Hospital Affiliated to Shanghai Jiaotong University School of Medicine: Shanghai Jiaotong University School of Medicine Xinhua Hospital https://orcid.org/0000-0003-1611-7273

Research Article

Keywords: Atherosclerosis, TFEB, Macrophage Foam cells, SUMOylation

Posted Date: June 27th, 2023

DOI: https://doi.org/10.21203/rs.3.rs-3034706/v1

Version of Record: A version of this preprint was published at Cellular and Molecular Life Sciences on November 11th, 2023. See the published version at https://doi.org/10.1007/s00018-023-04981-8.

Abstract

Atherosclerosis (AS) is a serious cardiovascular disease. One of its hallmarks is hyperlipidemia. Inhibiting the formation of macrophage foam cells is critical for alleviating AS. Transcription factor EB (TFEB) can limit the formation of macrophage foam cells by up-regulating lysosomal activity. We examined whether TFEB SUMOylation is involved in this progress during AS. In this study, we investigated the role of TFEB SUMOylation in macrophages in AS using TFEB SUMOylation deficiency *Ldlr*$^{-/-}$ (TFEB-KR: *Ldlr*$^{-/-}$) transgenic mice and TFEB-KR bone marrow–derived macrophages. We observed that TFEB-KR: *Ldlr*$^{-/-}$ atherosclerotic mice had thinner plaques and macrophages with higher lysosomal activity when compared to WT: *Ldlr*$^{-/-}$ mice. TFEB SUMOylation in macrophages decreased after oxidized low-density lipoprotein (OxLDL) treatment *in vitro*. Compared with wild type macrophages, TFEB-KR macrophages exhibited less lipid deposition after OxLDL treatment. Our study demonstrated that in AS, deSUMOylation of TFEB could inhibit the formation of macrophage foam cells through enhancing lysosomal biogenesis and autophagy, further reducing the accumulation of lipids in macrophages, and ultimately alleviating the development of AS. Thus, TFEB SUMOylation can be a switch to modulate macrophage foam cells formation and used as a potential target for AS therapy.

Introduction

Atherosclerosis (AS) is the most common cardiovascular disease in clinic. Hypercholesterolemia is a major risk factor for AS[1–4]. With the continuous improvement in living conditions, the incidence of AS has increased. Therefore, it is very important to study the pathogenesis of AS and explore potential therapeutic targets.

Macrophages play an important role in the early stage of AS. Recruited and differentiated macrophages can remove lipids deposited under vascular endothelium *via* lysosomal system, which is an important process to maintain the homeostasis of blood lipids [5, 6]. If macrophages take up too much lipids, it results in foam-like lipid formation in cytoplasm. These cells are called macrophage foam cells[7, 8]. We can slow down the formation of macrophage foam cells by enhancing their ability to process lipids and ultimately achieve the inhibition of AS.

Small ubiquitin-related modifiers (SUMOs) are a member of ubiquitin-like proteins[9]. Through a series of enzymatic reactions, SUMOs covalently bind to the substrate proteins and subsequently alter their functions. This post-translational modification is known as SUMOylation[10–12]. Many proteins can undergo SUMOylation. SUMOylation plays an important role in many aspects, such as regulating transcriptional activity, intracellular signal transduction, ensuring normal cell division, and maintaining the stability and integrity of genome[13].

As a transcription factor, transcription factor EB (TFEB) plays an important role in regulating lysosomal biogenesis and autophagy [14–17]. Several studies have considered TFEB as a valuable target for AS therapy[18–20]. According to recent reports, macrophages can metabolize cholesterol in cells using

lysosomal autophagy system and finally reduce the content of excess cholesterol in cells[21, 22]. In the AS model, the accumulation of atherosclerotic plaque in mice with TFEB conditionally overexpressed in macrophages was less and the content of proinflammatory factor interleukin-1β (IL-1β) in serum was also lower than that in wild type mice[5]. Therefore, TFEB is considered as a protective factor in the occurrence and development of atherosclerotic diseases. Although TFEB has been reported to be a SUMOylated protein [23], the function of TFEB SUMOylation in the development of AS remains unclear. In this study, we identified that TFEB SUMOylation was decreased after the stimulation of oxidized low-density lipoprotein (OxLDL) in macrophages, and TFEB-KR: *Ldlr*$^{-/-}$ mice exhibited milder atherosclerotic lesions with high cholesterol diet. Our study demonstrated that TFEB SUMOylation promoted the formation of macrophage foam cells by inhibiting lysosomal biogenesis and autophagy and eventually aggravated the development of AS. This indicated that targeting TFEB SUMOylation is a potential therapeutic strategy for AS.

Materials and methods

1. Plasmids and antibodies

GFP-TFEB, Flag-TFEB, HA-SSRP1, His-SUPT16H, SUMO1 were generated using standard cloning procedures (Vazyme Biotech Co.,Ltd). GFP-TFEB-K361R and Flag-TFEB-K361R were generated using site-directed mutagenesis (Strategene). Flag-SUMO1, HA-SUMO1 were gifts from Cheng laboratory. Antibodies against FLAG-M2, HA, and LC3 were purchased from Sigma, TFEB from Protein Tech, SUMO1 and LAMP1 from Abcam, ACTIN and His from Cell Signaling Technology.

2. Animal models

Animal studies were approved by the Animal Care and Use Committee from Xinhua Hospital, Affiliated to Medicine School of Shanghai Jiaotong University. Both TFEB-KR and *Ldlr*$^{-/-}$ mice were C57BL/6 background mice. *Ldlr*$^{-/-}$ mice were gifted from Professor Cheng's laboratory and TFEB-KR mice were generated by CRISPR/Cas9 gene targeting technology at Shanghai Bangyao Biotechnology Co. We used littermate derived, sex, age, and genetic background-matched mice in our experiments. TFEB-KR; *Ldlr*$^{-/-}$ mice were created by crossing mating TFEB-KR with *Ldlr*$^{-/-}$ mice to yield a double homozygote. Eight-weeks-old male littermates were used in the subsequent phenotype study. Atherosclerosis was induced by feeding 8-weeks-old WT: *Ldlr*$^{-/-}$ and TFEB-KR: *Ldlr*$^{-/-}$ littermates with a Western diet (Research diet) for 12 weeks.

3. Bone marrow transplantation

Eight-weeks-old male recipient mice were lethally irradiated with 900 rads irradiation on the day of transplantation. Bone marrow cells from the donor *Ldlr*$^{-/-}$ mice or *Ldlr*$^{-/-}$ mice with the whole body TFEB SUMOylation deficiency (TFEB-KR; *Ldlr*$^{-/-}$) were isolated and injected into each recipient mouse

intravenously. Four weeks later, the mice were fed with a Western diet for 12 weeks and subjected for atherosclerotic lesion analysis.

4. Histology

To determine lesion size, cryosections (8 μm) of the aortic root were stained with Oil Red O (Sigma). Corresponding sections on separate slides were also stained for monocyte/ macrophage content using a monoclonal rat MAC-3 antibody (BD), and lysosome using a rabbit polyclonal LAMP1 antibody (Abcam).

5. Cell culture

BMDMs were differentiated with M-CSF for 7 days. BMDMs,293T and RAW264.7 cells were cultured in DMEM (Hyclone) supplemented with 10% fetal bovine serum (Invitrogen) and 1% antibiotics (penicillin/streptomycin) (Invitrogen).

6. Immunoprecipitation and immunoblotting

BMDMs or transfected cells were lysed in radioimmune precipitation assay buffer (50 mMTris-HCl (pH 7.4), 400 mMNaCl, 1 mM EDTA, 1% Nonidet P-40, 0.1% SDS, 1% sodium deoxycholate, and a mixture of protease inhibitors) and cleared by centrifugation. Cleared cell lysates were incubated with 10 μl of anti-FLAG M2-agarose affinity gel (Sigma) or 2 μl of anti-SUMO1 (Abcam) with 10 μl of proteinA/G (Sigma) for 2 hrs. After extensive washing, beads were boiled at 100 ℃ for 10 min. Proteins were resolved by SDS-PAGE and transferred onto PVDF membranes (Millipore), followed by immunoblotting using corresponding antibodies according to the instructions of the manufacturer. Immunoblots were analyzed using the LAS-4000 system (Fujifilm).

7. RNA isolation and qPCR

Total RNA was isolated from cells by using Tripure isolation reagent (Roche). For mRNA analysis, an aliquot containing 2 μg of total RNA was reverse-transcribed using the cDNA synthesis kit (Takara). Real-time PCR was performed using SYBR Green PCR master mix (Applied Biosystems) and detected by the ABI Prism 7500 sequence detection system (Applied Biosystems). The primers for related genes are as follows:

CLCN7:

Forward Primer-CGCCAGTCTCATTCTGCACT,

Reverse Primer -GAGGATCGACTTCCGGGTC;

LAMP1:

Forward Primer-CAGCACTCTTTGAGGTGAAAAAC,

Reverse Primer -CCATTCGCAGTCTCGTAGGTG;

CTSB:

Forward Primer-CAGGCTGGACGCAACTTCTAC,

Reverse Primer-TCACCGAACGCAAC CCTTC;

CTSD:

Forward Primer-GCTTCCGGTCTTTGACAACCT,

Reverse Primer -CACCAAGCATTAGTTCTCCTCC;

ATG4b:

Forward Primer-CGGCACTTAGGTCGAGATTGG,

Reverse Primer -ACTCCCATTTGCGCTATCTGA;

ATG4d:

Forward Primer-AGGGGACAAACCCGTATCC,

Reverse Primer-CCATACTTGACGTTGTTCCAGG;

ATG5:

Forward Primer-TGTGCTTCGAGATGTGTGGTT,

Reverse Primer -ACCAACGTCAAATAGCTGACTC;

ATG9a:

Forward Primer-CCGAGGGGAGCAAATCACC,

Reverse Primer -TAGTCCACACAGCTAACCAGG;

CD36:

Forward Primer-ATGGGCTGTGATCGGAACTG,

Reverse Primer -TTTGCCACGTCATCTGGGTTT;

SCARB1:

Forward Primer-TTTGGAGTGGTAGTAAAAAGGGC,

Reverse Primer -TGACATCAGGGACTCAGAGTAG;

MSR1:

Forward Primer-TGGAGGAGAGAATCGAAAGCA,

Reverse Primer-CTGGACTGACGAAATCAAGGAA;

ABCG1:

Forward Primer-GTGGATGAGGTTGAGACAGACC,

Reverse Primer -CCTCGGGTACAGAGTAGGAAAG.

8. ChIP-qPCR assay

WT and TFEB-KR BMDMs were stimulated with OxLDL for 16h before crosslinking with 1% formaldehyde, and sonicated. Solubilized chromatin was immunoprecipitated with anti-TFEB antibody (Proteintech), washed, and then eluted. After crosslink reversal and proteinase K treatment, immunoprecipitated DNA was extracted with phenol-chloroform, ethanol precipitated. The DNA fragments were further analyzed by qPCR. The specific primers used to amplify Mcoln1 promoter region was as followed:

Forward primer-AGGGGCTCTGGGCTACC;

Reverse primer-GCCCGCCGCTGTC ACTG.

9. Flow cytometry

Cells were resuspended in 200 ml FACS buffer (PBS with 5% bovine calf serum) and placed on ice for 15 min to block. Cells were incubated with fluorescently labeled antibodies on ice in the dark for 20 min and then washed with PBS, centrifuged at 500 x g for 5 min, resuspended in 200 ml FACS buffer, and evaluated on a FACSCanto (Becton Dickinson) flow cytometer. Data were further analyzed using FlowJo software (Tree Star).

10. Protein digestion

100 μg of protein per condition was transferred into a new Eppendorf tube and the final volume was adjusted to 100 μL with 8 M urea. 2 μL of 0.5 M TCEP was added and the sample was incubated at 37℃ for 1 h, and then 4 μL of 1 M iodoacetamide was added to the sample and the incubation was last for 40 minutes protected from light at room temperature. After that, five volumes of -20℃ pre-chilled acetone was added to precipitate the proteins overnight at -20℃. The precipitates were washed by 1 mL pre-chilled 90% acetone aqueous solution for twice and then re-dissolved in 100 μL 100 mM TEAB. Sequence grade modified trypsin (Promega, Madison, WI) was added at the ratio of 1:50 (enzyme : protein, weight : weight) to digest the proteins at 37℃ overnight. The peptide mixture was desalted by C18 ZipTip and then lyophilized by SpeedVac.

11. nano-HPLC-MS/MS analysis

The sample was analyzed by on-line nanospray LC-MS/MS on Orbitrap Fusion™ mass spectrometer (Thermo Fisher Scientific, MA, USA)coupled to an EASY-nanoLC 1000 system(Thermo Fisher Scientific, MA, USA ．1 μL peptide was loaded (analytical column: Acclaim PepMap C18, 75 μm x 25 cm) and separated with a 60 min gradient. The column flow rate was maintained at 600 nL/min with the column temperature of 40°C. The electrospray voltage of 2 kV versus the inlet of the mass spectrometer was used. The chromatographic gradient is shown below (A: 0.1% formic acid in water; 0.1% formic acid in CAN):

Time	Duration	Flow [nl/min]	Mixture [%B]
00:00	00:00	600	5
03:00	03:00	600	8
37:00	34:00	600	20
51:00	14:00	600	30
52:00	01:00	600	90
60:00	08:00	600	90

The mass spectrometer was run under data dependent acquisition mode, and automatically switched between MS and MS/MS mode. The parameters was: (1) MS: scan range (m/z) = 350–1550; resolution = 60,000; AGC target = 4e5; maximum injection time = 50 ms; include charge states = 2–6 (2) HCD-MS/MS: resolution = 15,000; isolation window = 1.6; AGC target = 5e4; maximum injection time = 120 ms; collision energy = 35.

12. Luciferase assay

RAW264.7 cells in a 24-well plate were transiently transfected with indicated plasmids through FuGENE 6 transfection reagent (FuGENE). The cells were incubated for 24 hrs and then OxLDL (50 mg/ml) was used to stimulate the cells for 8 hours. Finally, Dual-Luciferase Reporter Assay System was used to assess the activity of the corresponding promoter (Promega). Lamp1-Luc, a LAMP1 promoter-luciferase construct, was performed as described previously[24].

13. Statistical analysis

Statistical analyses were performed with a 2-tailed unpaired Student’s t test. All data shown represent the results obtained from triplicated independent experiments with SEM (mean ± SD). The values of $P < 0.05$ were considered statistically significant.

Results

1. OxLDL stimulation reduced TFEB SUMOylation

TFEB has been reported to undergo SUMOylation and this modification has a key regulatory role in its transcriptional activity [23]. We confirmed this finding by co-transfecting TFEB and SUMO1 plasmids in 293T cells and observed that TFEB is indeed a SUMOylated protein (Figure-1A). Simultaneously, we identified that the SUMOylation site of human TFEB was lysine 361, since TFEB SUMOylation band was completely disappeared when lysine 361 was mutated to arginine (K361R) (Figure-1A). Although SUMOylation has proved a very important regulatory effect on the transcriptional activity of TFEB, the specific molecular mechanism under different stimulation conditions is not completely clear, including during macrophage foam cells formation.

To detect the SUMOylation of endogenous TFEB, we performed immune co-precipitation assay in bone marrow-derived macrophages (BMDMs). A band at approximately 100 kDa reflecting endogenous TFEB SUMOylation was detected (Figure-1B). WT and TFEB-KR BMDMs were confirmed by F4/80 and CD11b co-staining [25] (Figure-S1). To clarify the role of TFEB SUMOylation in AS, BMDMs were treated with OxLDL (50 mg/ml) for 24 hrs. The SUMOylation band of TFEB was significantly weakened after OxLDL stimulation (Figure-1C). These results suggested that TFEB SUMOylation was involved in the process of AS. Through protein sequence alignment, we found that TFEB SUMOylation site is highly conserved across various species (Figure-S2A). To further study the role of TFEB SUMOylation in the development of AS *in vivo*, we mapped the TFEB SUMOylation site in mice (Figure-1D) and constructed the TFEB SUMOylation deficiency mice (K346R) by using CRISPR/Cas9 base editing technology. We named it TFEB-KR mice (Figure-1E).

2. TFEB-KR: *Ldlr*$^{-/-}$ mice exhibited milder atherosclerotic lesions with high cholesterol diet

Since TFEB-KR mice had whole body TFEB SUMOylation deficiency, we performed bone marrow transplantation experiments in these mice prior to feeding them with a high cholesterol diet for 12 weeks (Figure-S3). The results revealed that TFEB-KR: *Ldlr*$^{-/-}$ mice exhibited less atherosclerotic plaques in the aorta when compared with the control mice (Figure-2A). The ratio of atherosclerotic plaques area to total aortic area in WT: *Ldlr*$^{-/-}$ mice was 20.1%, 19.3%, 26.0%, and 19.2% and that in TFEB-KR: *Ldlr*$^{-/-}$ mice was 12.3%, 16.3%, 16.2%, and 14.1%. In addition, we observed that the average aorta lesion in TFEB-KR: *Ldlr*$^{-/-}$ mice was approximately 30.3% less (Figure-2B) than that in the control mice. Furthermore, TFEB-KR: *Ldlr*$^{-/-}$ mice had thinner aortic sinus plaques and smaller atherosclerotic plaques (Figure-2C). MAC-3 is a glycoprotein that is expressed on the surface of monocytes and macrophages[26, 27]. Lysosomal associated membrane protein 1 (LAMP1) is a type 1 transmembrane protein that exists on the lysosomal membrane and can indirectly reflect the activity of lysosomes [28, 29]. TFEB-KR: *Ldlr*$^{-/-}$ mice exhibited stronger LAMP1 (red) but not MAC-3 (green) expression when compared with the control mice (Figure-2D/E). These results demonstrated that the number of macrophages infiltrating into atherosclerotic plaques was comparable between the two groups. However, macrophages in atherosclerotic plaques from TFEB-KR: *Ldlr*$^{-/-}$ mice exhibited higher lysosomal activity. Further, we measured the levels of triglyceride (TG), total cholesterol (TC), high-density lipoprotein (HDL), and low-density lipoprotein (LDL) in the serum collected from the two groups. The content of TG, TC, and LDL but not of HDL was slightly

higher in TFEB-KR: *Ldlr*$^{-/-}$ mice (Figure- 2H). This may be due to the higher lysosomal activity of macrophages in the plaques from TFEB-KR: *Ldlr*$^{-/-}$ mice, which can decompose and metabolize more lipids accumulated under the vascular endothelium. Further, we monitored the body weight between the two groups. No significant difference existed in body weight between the two groups even in the presence of western diet (Figure-2F). Moreover, the content of IL-1β, interleukin-4 (IL-4), and interleukin-6 (IL-6) was evaluated in the two groups from the AS model mice. TFEB-KR: *Ldlr*$^{-/-}$ mice exhibited lower IL-1β and higher IL-4 levels even though without significant difference. However, no difference was observed in terms of IL-6 secretion level (Figure-2G). These results indicated that TFEB-KR: *Ldlr*$^{-/-}$ mice was more resistant to inflammation. Collectively, we identified that TFEB SUMOylation plays an important role in the process of AS, and TFEB-KR: *Ldlr*$^{-/-}$ mice had stronger ability to resist AS.

3. TFEB SUMOylation inhibited lysosomal biogenesis and activity

Lyso-Tracker is a fluorescent probe labeled with weak alkalinity; therefore, it can selectively stain acidic lysosomes[30, 31]. Upon OxLDL stimulation, TFEB-KR BMDMs exhibited stronger Lyso-Tracker and LAMP1 staining signals and formed larger vacuoles when compared with WT BMDMs (Figure-3A/B). Further, quantitative analysis revealed higher MFI of Lyso-Tracker in TFEB-KR BMDMs after OxLDL treatment (Figure-3C/D). Real-time quantitative PCR detection revealed that genes associated with lysosomal biogenesis (*Clcn7*, *Lamp1*, *Ctsb*, and *Ctsd*) and autophagy (*Atg4b*, *Atg4d*, A*tg5* and *Atg9a*) were significantly upregulated in TFEB-KR BMDMs after OxLDL stimulation [32–36] (Figure-3E). The activity of cathepsin B (CTSB) can reflect the function of lysosome[37]. We observed that CTSB activity was approximately 26.1% higher in TFEB-KR BMDMs after OxLDL treatment (Figure-3G). LC3 is a class of microtubule associated protein, which plays a very important role in autophagy[38, 39]. We observed that the expression of LAMP1 and LC3 II was drastically increased in TFEB-KR BMDMs after OxLDL treatment (Figure-3F, Figure-S2B). These results indicated that TFEB-KR macrophages had higher lysosomal activity than wild type macrophages after OxLDL treatment.

4. TFEB-KR macrophages exhibited less lipid deposition upon OxLDL stimulation

BODIPY is used as a dye for natural oils and fats and a tracer for oils and other non-polar oils[40]. Oil red O and BODIPY staining revealed that lipid deposition was more pronounced in the wild type BMDMs (Figure-4A/B). We quantitatively analyzed the results of BODIPY staining using flow cytometry. The results revealed that the lipid content was approximately 31.6% less in TFEB-KR BMDMs (Figure-4C/D) than that in the WT group. Further, we measured the intracellular cholesterol content and observed that TFEB-KR BMDMs had less cholesterol (Figure-4E) than the WT group. These results suggested that TFEB-KR BMDMs had less lipid deposition after OxLDL stimulation.

In fact, the formation of macrophage foam cells is a way of metabolizing cholesterol by macrophages. The lipid metabolism process is very complex. It can be roughly divided into three steps: uptake, catabolism, and efflux of cholesterol[41–43]. Cholesterol uptake and efflux are mediated by a series of receptors. The major receptors related to cholesterol uptake include cluster of differentiation 36 (CD36),

scavenger receptor class B member 1 (Scarb1), and macrophages scavenger receptor 1 (Msr1) [44–46]. The main receptor of cholesterol efflux is ATP binding cassette subfamily G member 1 (Abcg1) [47]. Upon OxLDL stimulation at 16 hrs, the mRNA levels of the above receptors were elevated in both WT and TFEB-KR groups and there was no difference between the two groups (Figure-4F). Therefore, TFEB SUMOylation did not affect the expression of receptors related to cholesterol uptake and efflux in macrophages. Further, the cholesterol uptake capacity was assessed between the WT and TFEB-KR BMDMs, which was observed to be comparable in the two groups (Figure-4G). Finally, we observed that the cholesterol efflux of TFEB-KR BMDMs was significantly increased upon OxLDL stimulation at 6 hrs (Figure. 4H). These results suggested that because of stronger lysosomal function, less lipid deposition was present in TFEB-KR macrophages.

5. TFEB SUMOylation inhibited the transcriptional activity of TFEB by preventing its binding activity

Chloroquine (CQ) can be used as a lysosomal inhibitor. Alkaline CQ interacts with acidic lysosomes and inhibits the activity of lysosomes[48]. It has been reported that TFEB translocated into the cell nuclei with its transcriptional activity enhanced upon CQ stimulation[15]. We overexpressed WT and TFEB-KR plasmids in 293T cells. The cells were further stimulated with CQ for 15 hrs, and as a result, both WT and TFEB-KR proteins were able to translocate into the nuclei (Figure-5A), and there was no difference in the ratio of TFEB translocation into the nuclei between the two groups (Figure-5B). By analyzing the structure of TFEB, we observed that TFEB SUMOylation site was close to the DNA binding domain [49] (Figure-5C). Therefore, we used chromatin immuneprecipitation to test whether the binding ability of TFEB to its target genes was different between the two groups. Mucolipin-1 (Mcoln-1), also known as transient receptor potential channel muolipin-1 (Trpml1), is a classical target for TFEB and plays an important role in maintaining the biological function of lysosome [50]. We evaluated Mcoln-1 level in both groups with or without OxLDL stimulation. The binding ability of TFEB to *Mcoln-1* promoter was significantly increased in TFEB-KR macrophages upon stimulation (Figure-5D). These results indicated that TFEB SUMOylation inhibited its transcriptional activity by inhibiting its binding to its target genes.

6. TFEB SUMOylation inhibited the binding between TFEB and FACT complex to attenuate TFEB transcriptional activity

In order to further explore how TFEB SUMOylation affecting its transcriptional activity, we used mass spectrometry to find the key regulators affected by TFEB SUMOylation in this process. We overexpressed wild-type and mutant Flag-TFEB in 293T cells, and then enriched TFEB protein by immunoprecipitation (Figure-6A). Through mass spectrometry analysis, we found that TFEB SUMOylation affected its interaction with other proteins, among which the interaction with facilitates chromatin transcription (FACT) complex was the most affected (Figure-6B). FACT complex, a heterodimeric histone chaperone composed of structure specific recognition protein 1 (SSRP1) and SPT16 homolog, facilitates chromatin remodeling subunit (SUPT16H), mediates the disassembly and assembly of nucleosomes, thus improving the efficiency of transcription. A recent study showed that TFEB can regulate its transcriptional activity by binding to FACT, but the molecular mechanism is not fully understood[51]. To verify the

influence of TFEB SUMOylation on the interaction between TFEB and FACT complex observed in MS analysis, we used sodium arsenite ($NaAsO_2$) to stimulate 293T cells with overexpressed wild-type and mutant Flag-TFEB, respectively. $NaAsO_2$ is a kind of oxidative stress stimulator known to induce efficient translocation of TFEB from the cytosol to the nucleus. Our results showed that TFEB SUMOylation did inhibit the interaction between TFEB and FACT complex, and this inhibition effect was more obvious after TFEB was activated (Figure-6C). Finally, we used luciferase reporter gene experiment to verify that TFEB SUMOylation affected its transcriptional activity through the FACT complex during the process of macrophage foam cells formation. As previously described, LAMP1 is a target gene for TFEB and then we constructed a related reporter gene plasmid (Figure-6D). We used OxLDL to stimulate macrophages to imitate the process of foam cells formation in RAW264.7 cells. Our results showed that TFEB SUMOylation inhibited the activity of LAMP1 promoter during the process of macrophage foam cells formation, but this inhibition completely disappeared when the FACT complex and TFEB were co-transfected (Figure-6E). The above results showed that TFEB SUMOylation attenuated its transcriptional activity by inhibiting its interaction with FACT complex during the process of macrophage foam cells formation.

Discussion

Our results revealed that TFEB SUMOylation plays a very important role in the formation of macrophage foam cells and ultimately affects the development of AS. By analyzing AS animal models, we observed that macrophages with TFEB SUMOylation deficiency had higher lysosomal activity, which could deal with excessive lipid content and ultimately alleviate the development of AS. To identify the molecular mechanism underlying TFEB SUMOylation in the formation of macrophage foam cells, we used OxLDL to stimulate BMDMs to mimic AS conditions *in vitro*. We observed that after OxLDL treatment, TFEB SUMOylation was decreased and thus TFEB exhibited stronger binding ability to its target genes in TFEB-KR BMDMs. The higher transcriptional activity of TFEB led to TFEB-KR BMDMs presenting stronger lysosomal activity, which enabled BMDMs to process more cholesterol and ultimately alleviate lipid deposition. Therefore, the study herein demonstrated that under OxLDL stimulation, TFEB undergone deSUMOylation and deSUMOylated TFEB had stronger transcriptional activity and enhanced lipid degradation by enhancing lysosomal activity in macrophages, thereby inhibiting the formation of macrophage foam cells and ultimately alleviating the development of AS (Figure-7).

Macrophages play an important role in the early stage of AS, particularly in the formation of macrophage foam cells. Marcel *et al* reported that under LDL stimulation, the autophagy-lysosome system in macrophages is activated, which plays important roles in lipid processing and metabolism [7]. TFEB is a transcription factor that has an essential role in regulating lysosomal biogenesis and autophagy. A recent study by Razani *et al* reported that enhancing lysosomal activity by specifically overexpression of TFEB in macrophages can alleviate AS [5]. Therefore, TFEB is considered as a protective factor for AS.

In our study, we found that TFEB SUMOylation was significantly decreased after OxLDL stimulation. However, some questions remain to be addressed. First, OxLDL is a macromolecule complex that cannot

directly act on TFEB, it is unclear which signal specifically reduces the SUMOylation of TFEB upon the stimulation. Secondly, the molecular mechanism of TFEB deSUMOylation in macrophages remains unclear. SUMOylation is a dynamic and reversible process. The process of SUMOylation involves a series of enzymatic reactions mediated by E1/E2/E3. However, deSUMOylation is regulated by SUMO-specific proteases (SENPs) [52–55]. The decrease in TFEB SUMOylation may be due to the inhibition of the activity of one or more enzymes in E1/E2/E3 or the up-regulation of the activity or expression of the corresponding SENPs. There are six known SENPs, namely, SENP1, 2, 3, 5, 6, and 7 [55]. Which SENPs mediated the deSUMOylation of TFEB is yet to be investigated.

To the best of our knowledge, this is the first study on mice to report that TFEB-KR: *Ldlr*$^{-/-}$ mice had milder atherosclerosis onset and macrophages in plaques had stronger lysosomal activity. This is consistent with the study by Yang L *et al*, who reported that the high activity of TFEB in macrophages can make macrophages possess stronger lysosomal activity, which can alleviate the development of AS [56]. We measured IL-1β levels in atherosclerotic mice serum, which revealed that TFEB-KR: *Ldlr*$^{-/-}$ mice had lower IL-1β levels. This is consistent with the study by Razani B *et al* That the high activity of TFEB in macrophages render cells stronger lysosomal activity, thus reducing the IL-1β level and alleviating the development of AS[5]. However, it remains unclear why the decrease of IL-1β levels in atherosclerotic mice due to the high activity of TFEB in macrophages.

Finally, we observed that TFEB SUMOylation inhibited the transcriptional activity of TFEB by inhibiting its interaction with FACT complex. Since TFEB is a master regulator on lysosomal biogenesis and autophagy, the mechanisms for regulating TFEB activity should be sophiscated and diverse. Although we found that SUMOylation affected the interaction between TFEB and FACT complex, of course, it should affect its interaction with other proteins either. Therefore, there must be other mechanisms that affect the activity of TFEB through its SUMOylation. We speculated that there are several possible mechanisms: (1) TFEB SUMOylation may inhibit the binding ability of TFEB to its co-activators. (2) TFEB SUMOylation may enhance the binding ability of TFEB to its co-inhibitors. (3) TFEB SUMOylation may interact with other signaling pathways that can regulate the transcriptional activity of TFEB.

Collectively, our study demonstrated that TFEB SUMOylation is involved in the pathogenesis of AS by regulating the formation of macrophage foam cells. TFEB SUMOylation promoted the formation of macrophage foam cells by inhibiting lysosomal biogenesis and autophagy and eventually aggravated the development of AS. Therefore, TFEB SUMOylation in macrophages might be applied as a novel target for AS therapy. Drugs that can reduce TFEB SUMOylation in macrophage foam cells should be developed in the future, to enhance the ability of macrophages to process lipids, thereby alleviating or inhibiting the development of AS.

Abbreviations

AS, Atherosclerosis; TFEB, Transcription factor EB; SUMOs, Small ubiquitin-like modifiers; SENPs, SUMO specific Peptidases; OxLDL, oxidized low-density lipoprotein; IL-1b, interleukin-1b; LAMP1, Lysosomal

associated membrane protein 1; CLCN7, chloride channel, voltage-sensitive 7; TG, Triglyceride; TC, Total Cholesterol; HDL, High-density lipoprotein; LDL, Low-density lipoprotein; IL-4, Interleukin-4; IL-6, Interleukin-6; CTSB, Cathepsin B; CTSD, Cathepsin D; CD36, Cluster of differentiation 36; Scarb1, Scavenger receptor class B member 1; Msr1, Macrophages scavenger receptor 1; Abcg1, ATP binding cassette subfamily G member 1; CQ, Chloroquine; Mcoln-1, Mucolipin-1; Trpml1, Transient receptor potential channel muolipin-1;FACT, facilitates chromatin transcription; SSRP1, structure specific recognition protein 1; SUPT16H, SPT16 homolog, facilitates chromatin remodeling subunit; NaAsO2, sodium arsenite.

Declarations

Author Contributions: R.C. and T.T. designed and conceived the project, provided the concept, contributed to the manuscript and supervised the research. K.Z.W. designed and performed experiments, analyzed and interpreted the data, and prepared the manuscript. R.C. and T.T. designed experiments and edited the manuscript. L.F.W.,W.Z. and G.L.H. assisted with BMDM preparation and performed flow cytometry. All authors analyzed and interpreted the data, revised for critical intellectual content and approved the final manuscript. All authors have read and agreed to the published version of the manuscript.

Acknowledgments We thank Prof. Jinke Cheng for his excellent technical assistance. We thank Bullet Edits Limited for the linguistic editing and proofreading of the manuscript.No sources of financial support for the conduct of the research and/or preparation of the article. No conflicts of interest to disclosure.

Funding This research was funded by National Natural Science Foundation of China (82002937, 82000904).

Data availability All the data supporting the findings of this study are available within the paper. Data will be made available on reasonable request, not applicable for material.

Conflict of interest The funders had no conflicts of interest in the design of the study; in the collection, analysis or interpretation of data; in the writing of the manuscript, or in the decision to publish the results.

Ethics approval Animal studies were approved by the Animal Care and Use Committee from Xinhua Hospital, Affiliated to Medicine School of Shanghai Jiaotong University.

Consent to participate Not applicable.

Consent for publication All authors have been involved in writing the manuscript and consented to publication.

References

1. Wang HH, Garruti G, Liu M, Portincasa P, Wang DQ (2017) Cholesterol and Lipoprotein Metabolism and Atherosclerosis: Recent Advances In reverse Cholesterol Transport. Ann Hepatol 16:s27–s42

2. Que X, Hung MY, Yeang C, Gonen A, Prohaska TA, Sun X, Diehl C, Maatta A, Gaddis DE, Bowden K, Pattison J, MacDonald JG, Yla-Herttuala S, Mellon PL, Hedrick CC, Ley K, Miller YI, Glass CK, Peterson KL, Binder CJ, Tsimikas S, Witztum JL (2018) Oxidized phospholipids are proinflammatory and proatherogenic in hypercholesterolaemic mice. Nature 558:301–306
3. Tontonoz P, Wu X, Jones M, Zhang Z, Salisbury D, Sallam T (2017) Long Noncoding RNA Facilitated Gene Therapy Reduces Atherosclerosis in a Murine Model of Familial Hypercholesterolemia. Circulation 136:776–778
4. Bjorkegren JLM, Lusis AJ (2022) Atherosclerosis: Recent developments. Cell 185:1630–1645
5. Sergin I, Evans TD, Zhang X, Bhattacharya S, Stokes CJ, Song E, Ali S, Dehestani B, Holloway KB, Micevych PS, Javaheri A, Crowley JR, Ballabio A, Schilling JD, Epelman S, Weihl CC, Diwan A, Fan D, Zayed MA, Razani B (2017) Exploiting macrophage autophagy-lysosomal biogenesis as a therapy for atherosclerosis. Nat Commun 8:15750
6. Edgar L, Akbar N, Braithwaite AT, Krausgruber T, Gallart-Ayala H, Bailey J, Corbin AL, Khoyratty TE, Chai JT, Alkhalil M, Rendeiro AF, Ziberna K, Arya R, Cahill TJ, Bock C, Laurencikiene J, Crabtree MJ, Lemieux ME, Riksen NP, Netea MG, Wheelock CE, Channon KM, Ryden M, Udalova IA, Carnicer R, Choudhury RP (2021) Hyperglycemia Induces Trained Immunity in Macrophages and Their Precursors and Promotes Atherosclerosis. Circulation 144:961–982
7. Ouimet M, Franklin V, Mak E, Liao X, Tabas I, Marcel YL (2011) Autophagy regulates cholesterol efflux from macrophage foam cells via lysosomal acid lipase. Cell Metab 13:655–667
8. Robichaud S, Fairman G, Vijithakumar V, Mak E, Cook DP, Pelletier AR, Huard S, Vanderhyden BC, Figeys D, Lavallee-Adam M, Baetz K, Ouimet M (2021) Identification of novel lipid droplet factors that regulate lipophagy and cholesterol efflux in macrophage foam cells. Autophagy 17:3671–3689
9. Pickart CM (2001) Mechanisms underlying ubiquitination. Annu Rev Biochem 70:503–533
10. Zhao X (2018) SUMO-Mediated Regulation of Nuclear Functions and Signaling Processes. Mol Cell 71:409–418
11. Ma G, Li S, Han Y, Li S, Yue T, Wang B, Jiang J (2016) Regulation of Smoothened Trafficking and Hedgehog Signaling by the SUMO Pathway. Dev Cell 39:438–451
12. Conti L, Nelis S, Zhang C, Woodcock A, Swarup R, Galbiati M, Tonelli C, Napier R, Hedden P, Bennett M, Sadanandom A (2014) Small Ubiquitin-like Modifier protein SUMO enables plants to control growth independently of the phytohormone gibberellin. Dev Cell 28:102–110
13. Wilson VG (2017) Introduction to Sumoylation. Adv Exp Med Biol 963:1–12
14. Yang M, Liu E, Tang L, Lei Y, Sun X, Hu J, Dong H, Yang SM, Gao M, Tang B (2018) Emerging roles and regulation of MiT/TFE transcriptional factors. Cell Commun Signal 16:31
15. Tol MJ, van der Lienden MJC, Gabriel TL, Hagen JJ, Scheij S, Veenendaal T, Klumperman J, Donker-Koopman WE, Verhoeven AJ, Overkleeft H, Aerts JM, Argmann CA, van Eijk M (2018) HEPES activates a MiT/TFE-dependent lysosomal-autophagic gene network in cultured cells: A call for caution. Autophagy 14:437–449

16. Puertollano R, Ferguson SM, Brugarolas J, Ballabio A (2018) The complex relationship between TFEB transcription factor phosphorylation and subcellular localization, EMBO J 37
17. Tao H, Yancey PG, Blakemore JL, Zhang Y, Ding L, Jerome WG, Brown JD, Vickers KC, Linton MF (2021) Macrophage SR-BI modulates autophagy via VPS34 complex and PPARalpha transcription of Tfeb in atherosclerosis, J Clin Invest 131
18. Fang S, Wan X, Zou X, Sun S, Hao X, Liang C, Zhang Z, Zhang F, Sun B, Li H, Yu B (2021) Arsenic trioxide induces macrophage autophagy and atheroprotection by regulating ROS-dependent TFEB nuclear translocation and AKT/mTOR pathway. Cell Death Dis 12:88
19. Jeong SJ, Stitham J, Evans TD, Zhang X, Rodriguez-Velez A, Yeh YS, Tao J, Takabatake K, Epelman S, Lodhi IJ, Schilling JD, DeBosch BJ, Diwan A, Razani B (2021) Trehalose causes low-grade lysosomal stress to activate TFEB and the autophagy-lysosome biogenesis response. Autophagy 17:3740–3752
20. Chen Z, Ouyang C, Zhang H, Gu Y, Deng Y, Du C, Cui C, Li S, Wang W, Kong W, Chen J, Cai J, Geng B (2022) Vascular smooth muscle cell-derived hydrogen sulfide promotes atherosclerotic plaque stability via TFEB (transcription factor EB)-mediated autophagy, *Autophagy*, 1–18
21. Li M, Wang Z, Wang P, Li H, Yang L (2021) TFEB: A Emerging Regulator in Lipid Homeostasis for Atherosclerosis. Front Physiol 12:639920
22. Zhao J, Hu B, Xiao H, Yang Q, Cao Q, Li X, Zhang Q, Ji A, Song S (2021) Fucoidan reduces lipid accumulation by promoting foam cell autophagy via TFEB. Carbohydr Polym 268:118247
23. Miller AJ, Levy C, Davis IJ, Razin E, Fisher DE (2005) Sumoylation of MITF and its related family members TFE3 and TFEB. J Biol Chem 280:146–155
24. Qiu S, Liang Z, Wu Q, Wang M, Yang M, Chen C, Zheng H, Zhu Z, Li L, Yang G (2022) Hepatic lipid accumulation induced by a high-fat diet is regulated by Nrf2 through multiple pathways. FASEB J 36:e22280
25. Endo-Umeda K, Nakashima H, Komine-Aizawa S, Umeda N, Seki S, Makishima M (2018) Liver X receptors regulate hepatic F4/80 (+) CD11b(+) Kupffer cells/macrophages and innate immune responses in mice. Sci Rep 8:9281
26. Wang J, Sjoberg S, Tia V, Secco B, Chen H, Yang M, Sukhova GK, Shi GP (2013) Pharmaceutical stabilization of mast cells attenuates experimental atherogenesis in low-density lipoprotein receptor-deficient mice. Atherosclerosis 229:304–309
27. Breder I, Coope A, Arruda AP, Razolli D, Milanski M, Dorighello Gde G, de Oliveira HC, Velloso LA (2010) Reduction of endoplasmic reticulum stress–a novel mechanism of action of statins in the protection against atherosclerosis. Atherosclerosis 212:30–31
28. Unuma K, Aki T, Funakoshi T, Hashimoto K, Uemura K (2015) Extrusion of mitochondrial contents from lipopolysaccharide-stimulated cells: Involvement of autophagy. Autophagy 11:1520–1536
29. Rusmini P, Cortese K, Crippa V, Cristofani R, Cicardi ME, Ferrari V, Vezzoli G, Tedesco B, Meroni M, Messi E, Piccolella M, Galbiati M, Garre M, Morelli E, Vaccari T, Poletti A (2019) Trehalose induces

autophagy via lysosomal-mediated TFEB activation in models of motoneuron degeneration. Autophagy 15:631–651

30. Ben M, Ajjaji K, Chorlay D, Vanni A, Foret S, L., Thiam AR (2017) ER Membrane Phospholipids and Surface Tension Control Cellular Lipid Droplet Formation. Dev Cell 41:591–604e7
31. Brancucci NMB, Gerdt JP, Wang C, De Niz M, Philip N, Adapa SR, Zhang M, Hitz E, Niederwieser I, Boltryk SD, Laffitte MC, Clark MA, Gruring C, Ravel D, Soares B, Demas A, Bopp A, Rubio-Ruiz S, Conejo-Garcia B, Wirth A, Gendaszewska-Darmach DF, Duraisingh E, Adams MT, Voss JH, Waters TS, Jiang AP, Clardy RHY, J., Marti M (2017) Lysophosphatidylcholine Regulates Sexual Stage Differentiation in the Human Malaria Parasite Plasmodium falciparum. Cell 171:1532–1544e15
32. Gayle S, Landrette S, Beeharry N, Conrad C, Hernandez M, Beckett P, Ferguson SM, Mandelkern T, Zheng M, Xu T, Rothberg J, Lichenstein H (2017) Identification of apilimod as a first-in-class PIKfyve kinase inhibitor for treatment of B-cell non-Hodgkin lymphoma. Blood 129:1768–1778
33. Zhang J, Wang J, Zhou Z, Park JE, Wang L, Wu S, Sun X, Lu L, Wang T, Lin Q, Sze SK, Huang D, Shen HM (2018) Importance of TFEB acetylation in control of its transcriptional activity and lysosomal function in response to histone deacetylase inhibitors. Autophagy 14:1043–1059
34. Parousis A, Carter HN, Tran C, Erlich AT, Moosavi M, Pauly ZS, M., Hood DA (2018) Contractile activity attenuates autophagy suppression and reverses mitochondrial defects in skeletal muscle cells. Autophagy 14:1886–1897
35. Ni Z, Gong Y, Dai X, Ding W, Wang B, Gong H, Qin L, Cheng P, Li S, Lian J, He F (2015) AU4S: a novel synthetic peptide to measure the activity of ATG4 in living cells, *Autophagy.* 11, 403 – 15
36. Zhou C, Ma K, Gao R, Mu C, Chen L, Liu Q, Luo Q, Feng D, Zhu Y, Chen Q (2017) Regulation of mATG9 trafficking by Src- and ULK1-mediated phosphorylation in basal and starvation-induced autophagy. Cell Res 27:184–201
37. Man SM, Kanneganti TD (2016) Regulation of lysosomal dynamics and autophagy by CTSB/cathepsin B. Autophagy 12:2504–2505
38. Zhou J, Wang Z, Wang X, Li X, Zhang Z, Fan B, Zhu C, Chen Z (2018) Dicot-specific ATG8-interacting ATI3 proteins interact with conserved UBAC2 proteins and play critical roles in plant stress responses. Autophagy 14:487–504
39. Frudd K, Burgoyne T, Burgoyne JR (2018) Oxidation of Atg3 and Atg7 mediates inhibition of autophagy. Nat Commun 9:95
40. Qiu B, Simon MC (2016) BODIPY 493/503 Staining of Neutral Lipid Droplets for Microscopy and Quantification by Flow Cytometry, Bio Protoc 6
41. Kothari V, Bornfeldt KE (2017) Liver Kinase B1 Links Macrophage Metabolism Sensing and Atherosclerosis. Circ Res 121:1024–1026
42. Childs BG, Baker DJ, Wijshake T, Conover CA, Campisi J, van Deursen JM (2016) Senescent intimal foam cells are deleterious at all stages of atherosclerosis. Science 354:472–477
43. Toledo JD, Garda HA, Cabaleiro LV, Cuellar A, Pellon-Maison M, Gonzalez-Baro MR, Gonzalez MC (2013) Apolipoprotein A-I Helsinki promotes intracellular acyl-CoA cholesterol acyltransferase (ACAT)

protein accumulation. Mol Cell Biochem 377:197–205

44. Conrad KS, Cheng TW, Ysselstein D, Heybrock S, Hoth LR, Chrunyk BA, Ende A, Krainc CW, Schwake D, Saftig M, Liu P, Qiu S, X., Ehlers MD (2017) Lysosomal integral membrane protein-2 as a phospholipid receptor revealed by biophysical and cellular studies, *Nat Commun.* 8, 1908
45. Sorci-Thomas MG, Thomas MJ (2016) Microdomains, Inflammation, and Atherosclerosis. Circ Res 118:679–691
46. An D, Hao F, Zhang F, Kong W, Chun J, Xu X, Cui MZ (2017) CD14 is a key mediator of both lysophosphatidic acid and lipopolysaccharide induction of foam cell formation. J Biol Chem 292:14391–14400
47. Ma W, Ding H, Gong X, Liu Z, Lin Y, Zhang Z, Lin G (2015) Methyl protodioscin increases ABCA1 expression and cholesterol efflux while inhibiting gene expressions for synthesis of cholesterol and triglycerides by suppressing SREBP transcription and microRNA 33a/b levels. Atherosclerosis 239:566–570
48. Maulucci G, Chiarpotto M, Papi M, Samengo D, Pani G, De Spirito M (2015) Quantitative analysis of autophagic flux by confocal pH-imaging of autophagic intermediates, Autophagy 11, 1905–16
49. Nabar NR, Kehrl JH (2017) The Transcription Factor EB Links Cellular Stress to the Immune Response. Yale J Biol Med 90:301–315
50. Zhang X, Cheng X, Yu L, Yang J, Calvo R, Patnaik S, Hu X, Gao Q, Yang M, Lawas M, Delling M, Marugan J, Ferrer M, Xu H (2016) MCOLN1 is a ROS sensor in lysosomes that regulates autophagy. Nat Commun 7:12109
51. Jeong E, Martina JA, Contreras PS, Lee J, Puertollano R (2022) The FACT complex facilitates expression of lysosomal and antioxidant genes through binding to TFEB and TFE3. Autophagy 18:2333–2349
52. Wei B, Huang C, Liu B, Wang Y, Xia N, Fan Q, Chen GQ, Cheng J (2018) Mitotic Phosphorylation of SENP3 Regulates DeSUMOylation of Chromosome-Associated Proteins and Chromosome Stability. Cancer Res 78:2171–2178
53. Xu Z, Chan HY, Lam WL, Lam KH, Lam LS, Ng TB, Au SW (2009) SUMO proteases: redox regulation and biological consequences. Antioxid Redox Signal 11:1453–1484
54. Nayak A, Muller S (2014) SUMO-specific proteases/isopeptidases: SENPs and beyond. Genome Biol 15:422
55. Mukhopadhyay D, Dasso M (2007) Modification in reverse: the SUMO proteases. Trends Biochem Sci 32:286–295
56. Li X, Zhang X, Zheng L, Kou J, Zhong Z, Jiang Y, Wang W, Dong Z, Liu Z, Han X, Li J, Tian Y, Zhao Y, Yang L (2016) Hypericin-mediated sonodynamic therapy induces autophagy and decreases lipids in THP-1 macrophage by promoting ROS-dependent nuclear translocation of TFEB. Cell Death Dis 7:e2527

Figures

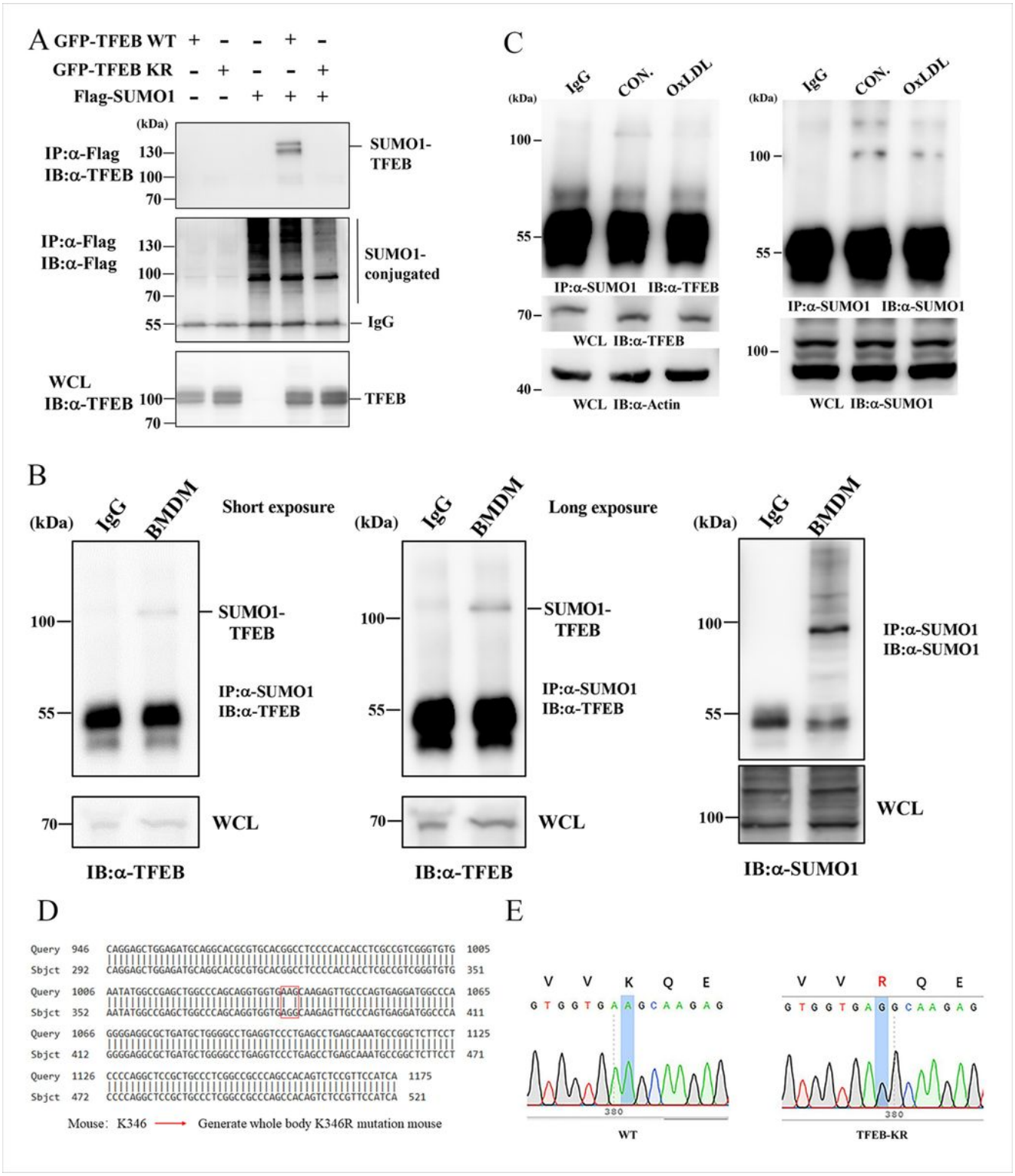

Figure 1

OxLDL stimulation reduced TFEB SUMOylation.

A: Human TFEB was SUMOylated at K361. Cell lysates from 293T cells transfected with the indicated plasmids were immunoprecipitated with anti-Flag beads. The precipitated proteins or lysates were immunoblotted with anti-Flag or anti-TFEB antibodies.

B: Endogenous TFEB could be SUMOylated in bone marrow–derived macrophages. BMDMs were immunoprecipitated with anti-SUMO1 antibody. The precipitated proteins or lysates were immunoblotted with anti-SUMO1 or anti-TFEB antibodies.

C: TFEB SUMOylation was decreased after OxLDL treatment. BMDMs were treated with OxLDL (50 mg/ml) for 24 hrs. The alteration of TFEB SUMOylation was detected using immunoprecipitation; n = 3.

D: Using the BLAST function from the PubMed database, compare the DNA sequences of TFEB and identify the SUMOylation modification sites.

E: Construction of genetic mouse model with the whole body TFEB SUMOylation deficiency (TFEB-KR, K346R) and the results were confirmed through PCR sequencing.

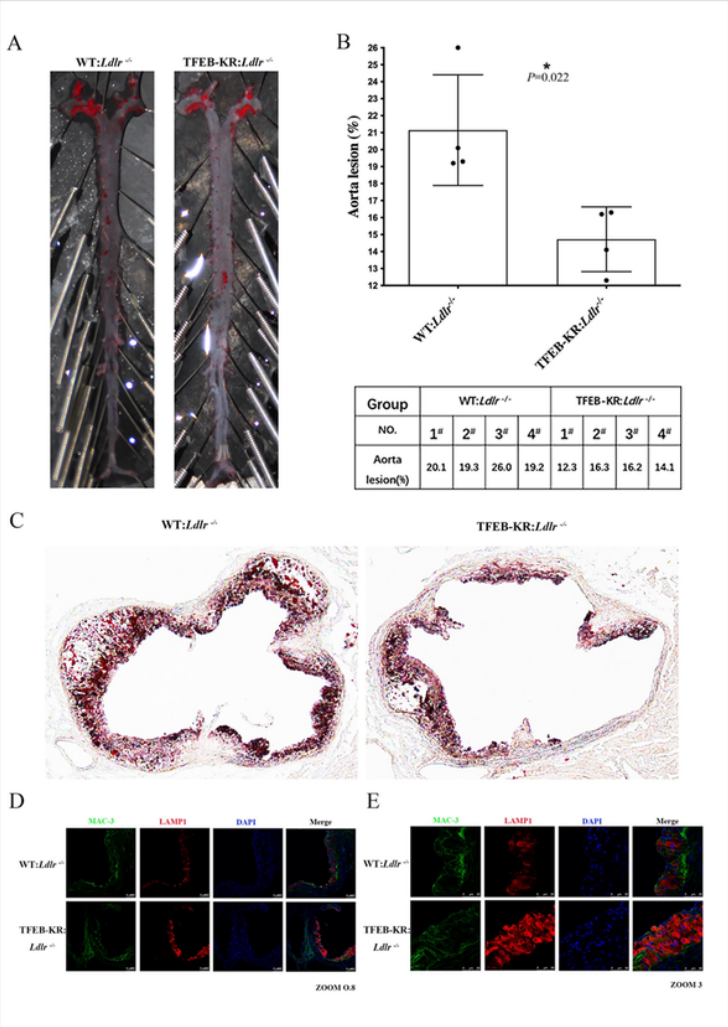

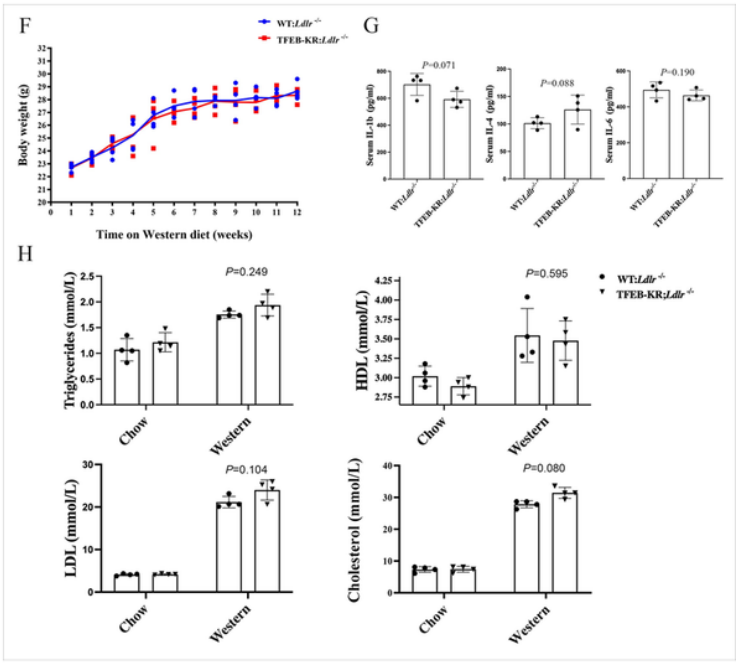

Figure 2

TFEB-KR: *Ldlr*$^{-/-}$ mice exhibited milder atherosclerotic lesions with high cholesterol diet.

A: Representative images of en face oil red O staining of aortas from WT: *Ldlr*$^{-/-}$ and TFEB-KR: *Ldlr*$^{-/-}$ littermates; n = 4.

B: Quantitative analysis of the ratio of lesion areas to total aortic areas in each mouse; n = 4.

C: Representative images of cross-sections of the aortic sinus stained with oil red O; n = 4.

D. The staining of Lamp1 in Mac-3-positive macrophages in lesions of WT: *Ldlr*$^{-/-}$ and TFEB-KR: *Ldlr*$^{-/-}$ mice; n = 4 (ZOOM 0.8).

E. The staining of Lamp1 in Mac-3-positive macrophages in lesions of WT: *Ldlr*$^{-/-}$ and TFEB-KR: *Ldlr*$^{-/-}$ mice; n = 4 (ZOOM 3).

F. Body weight of WT: *Ldlr*$^{-/-}$ and TFEB-KR: *Ldlr*$^{-/-}$ mice on a normal chow diet or a western diet; n = 4.

G. Detection of inflammatory factors amounts in WT: *Ldlr*$^{-/-}$ and TFEB-KR: *Ldlr*$^{-/-}$ mice after feeding western diet; n = 4.

H. Cholesterol levels, and lipoprotein profiles of WT: *Ldlr*$^{-/-}$ and TFEB-KR: *Ldlr*$^{-/-}$ mice on a normal chow diet or a western diet; n = 4.

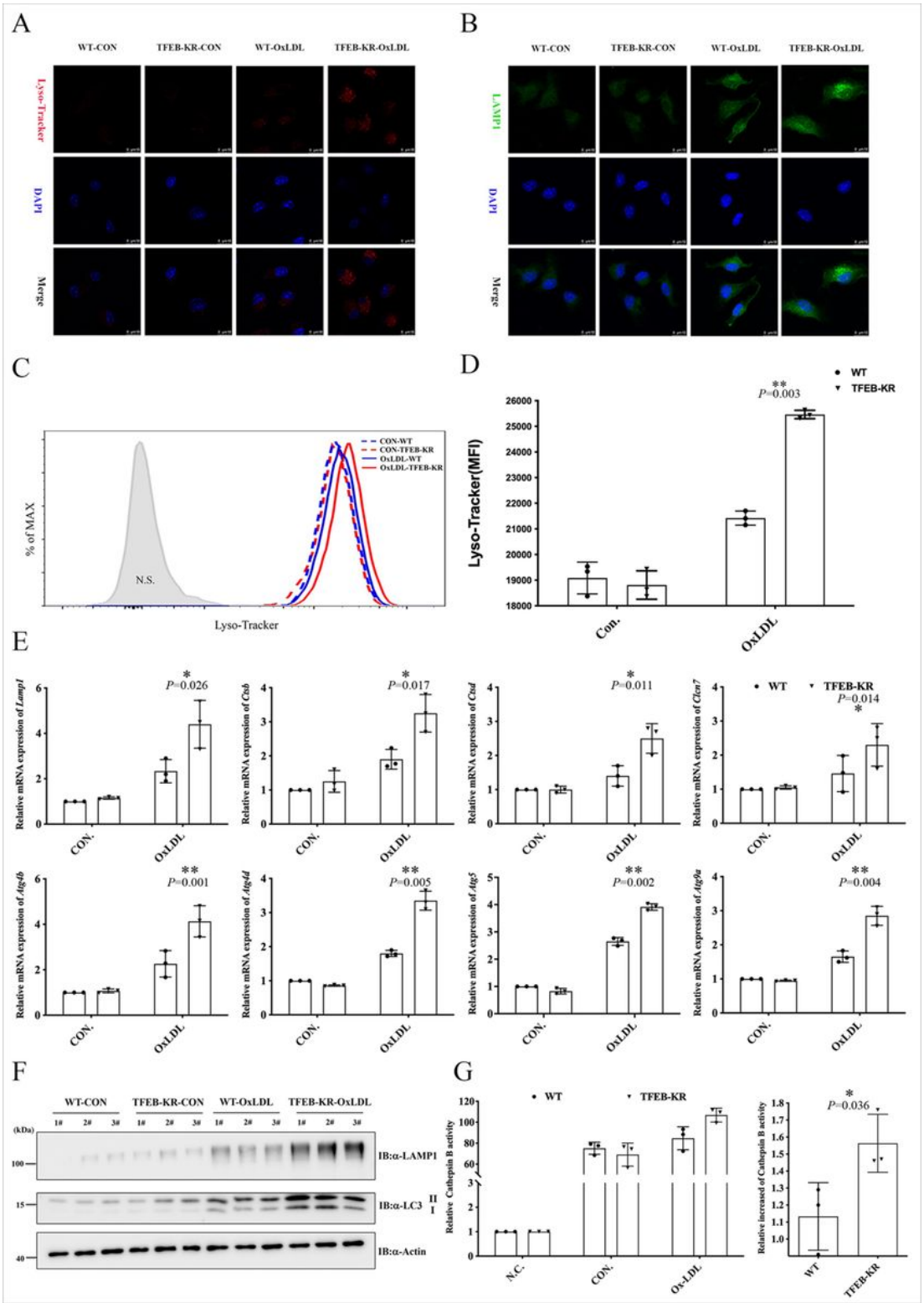

Figure 3

TFEB SUMOylation inhibited lysosomal biogenesis and activity.

A: Under OxLDL stimulation, Lyso-Tracker Red staining was more pronounced in TFEB-KR BMDMs. WT and TFEB-KR BMDMs were treated with OxLDL (50mg/ml) for 24 hours, followed by Lyso-Tracker Red staining; n = 3.

B: Under OxLDL stimulation, LAMP1 staining was more pronounced in TFEB-KR BMDMs. WT and TFEB-KR BMDMs were treated with OxLDL (50mg/ml) for 24 hours, followed by LAMP1 staining; n = 3.

C: Under OxLDL stimulation, Lyso-Tracker Red staining was more pronounced in TFEB-KR BMDMs. WT and TFEB-KR BMDMs were treated with OxLDL (50mg/ml) for 24 hours, followed by Lyso-Tracker Red staining, which was quantified using flow cytometry; n = 3.

D: Quantitative analysis of the Lyso-Tracker MFI after OxLDL treatment in WT and TFEB-KR BMDMs; n = 3.

E: Under OxLDL stimulation, the expression of TFEB target genes were increased more significantly in TFEB-KR BMDMs. WT and TFEB-KR BMDMs were treated with OxLDL (50mg/ml) for 16 hours and then relative mRNA levels of TFEB target genes were assessed by Real-time quantitative PCR; n = 3.

F: Under OxLDL stimulation, the protein levels of LAMP1 and LC3 were more significantly in TFEB-KR BMDMs. WT and TFEB-KR BMDMs were treated with OxLDL (50mg/ml) for 24 hours and then the cells lysates were immunoblotted with anti-LAMP1 / anti-LC3 or anti-Actin antibodies; n = 3.

G: Under OxLDL stimulation, the activity of cathepsin B was higher in TFEB-KR BMDMs. WT and TFEB-KR BMDMs were treated with OxLDL (50mg/ml) for 24 hours and then the activity of cathepsin B was measured; n = 3.

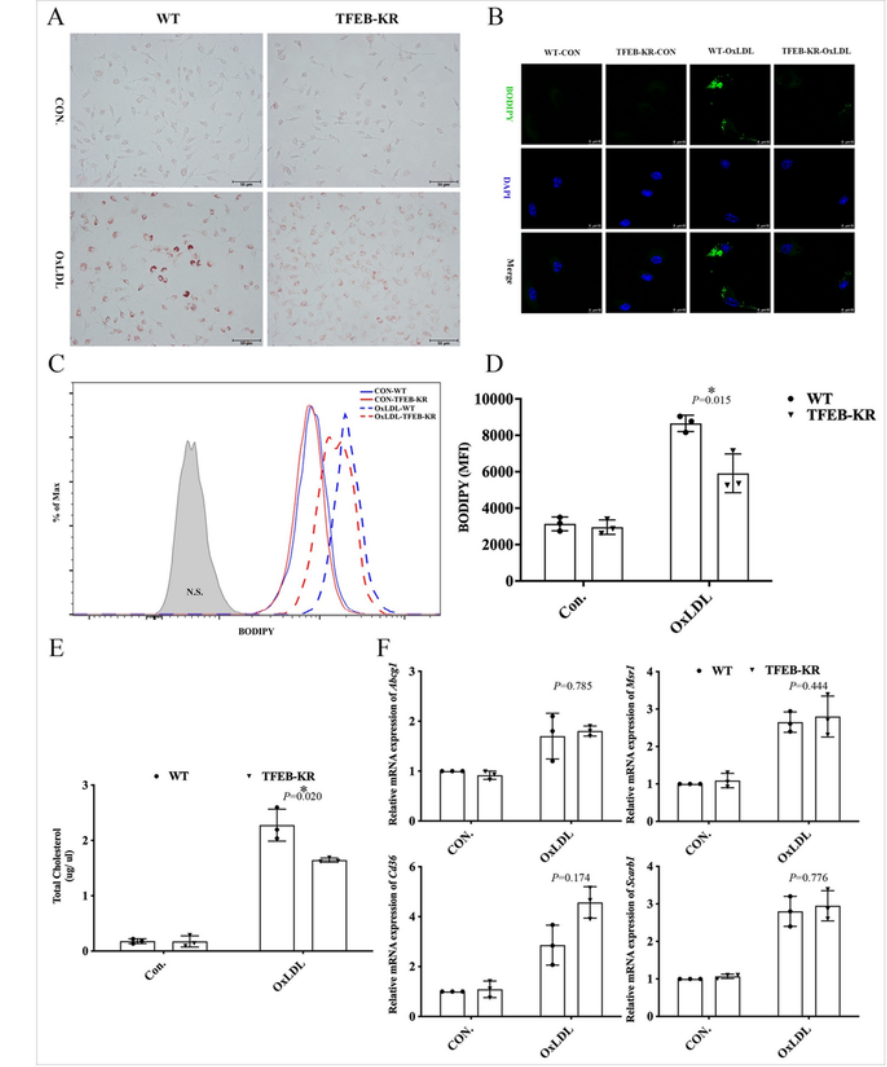

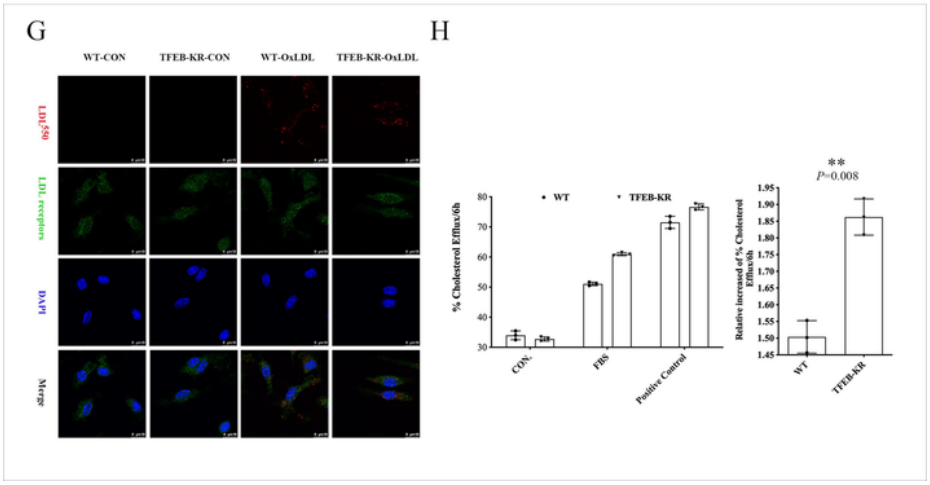

Figure 4

TFEB-KR macrophages exhibited less lipid deposition upon OxLDL stimulation.

A: TFEB-KR BMDMs inhibited the formation of macrophage foam cells. WT and TFEB-KR BMDMs were incubated with OxLDL (50mg/ml) for 24 hrs, fixed, and stained with oil red O; n = 3.

B: Under OxLDL stimulation, there was less lipid deposition in TFEB-KR BMDMs. WT and TFEB-KR BMDMs were incubated with OxLDL (50mg/ml) for 24 hrs, LDs were stained using BODIPY and observed using immunofluorescence; n = 3.

C: Under OxLDL stimulation, there was less lipid deposition in TFEB-KR BMDMs. WT and TFEB-KR BMDMs were incubated with OxLDL (50mg/ml) for 24 hrs, LDs were stained using BODIPY and quantified using flow cytometry; n = 3.

D: Quantitative analysis of the BODIPY MFI after OxLDL treatment in WT and TFEB-KR BMDMs; n = 3.

E: Under OxLDL stimulation, TFEB-KR BMDMs had lower total cholesterol levels. WT and TFEB-KR BMDMs were incubated with OxLDL (50mg/ml) for 24 hrs and the content of total cholesterol in WT and TFEB-KR BMDMs was assessed before or after OxLDL treatment; n = 3.

F: TFEB SUMOylation did not significantly alter the expression of main scavenger receptors in macrophages after OxLDL treatment. WT and TFEB-KR BMDMs were treated with OxLDL (50mg/ml) for 16 hours and then relative mRNA levels of main scavenger receptors were assessed by Real-time quantitative PCR; n = 3.

G: TFEB SUMOylation did not affect LDL uptake in WT and TFEB-KR BMDMs; n = 3.

H: Under OxLDL stimulation, the cholesterol efflux was significantly increased in TFEB-KR BMDMs. Analysis of cholesterol efflux in WT and TFEB-KR BMDMs after OxLDL treatment through cholesterol efflux assay kit; n = 3.

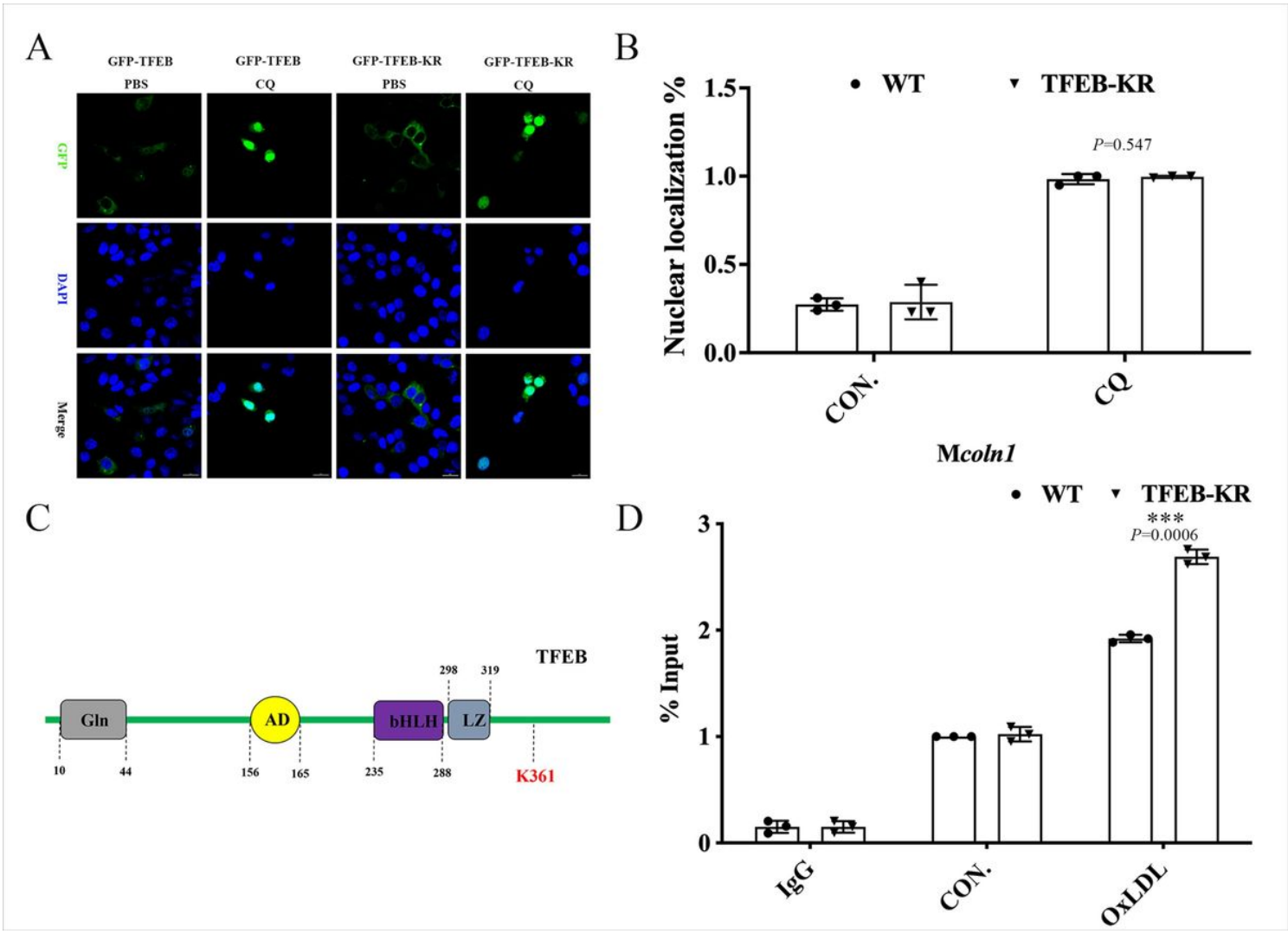

Figure 5

TFEB SUMOylation inhibited its transcriptional activity by preventing the binding activity.

A: TFEB SUMOylation did not affect its nuclear localization. Wild-type and TFEB-KR plasmids labeled with GFP were transfected into 293T cells respectively and then stimulated the cells with chloroquine for 15 hours to observe the nuclear entry of TFEB n = 3.

B. Quantitative analysis of the ratio of TFEB entering the nuclei in WT and TFEB-KR groups; n=3.

C: The structure of TFEB.

D: Under OxLDL stimulation, TFEB SUMOylation inhibited its transcriptional activity. WT and TFEB-KR BMDMs were treated with OxLDL (50mg/ml) for 16 hours and then the binding ability of TFEB and its target gene MCOLN1 was measured by chromatin immunoprecipitation; n = 3.

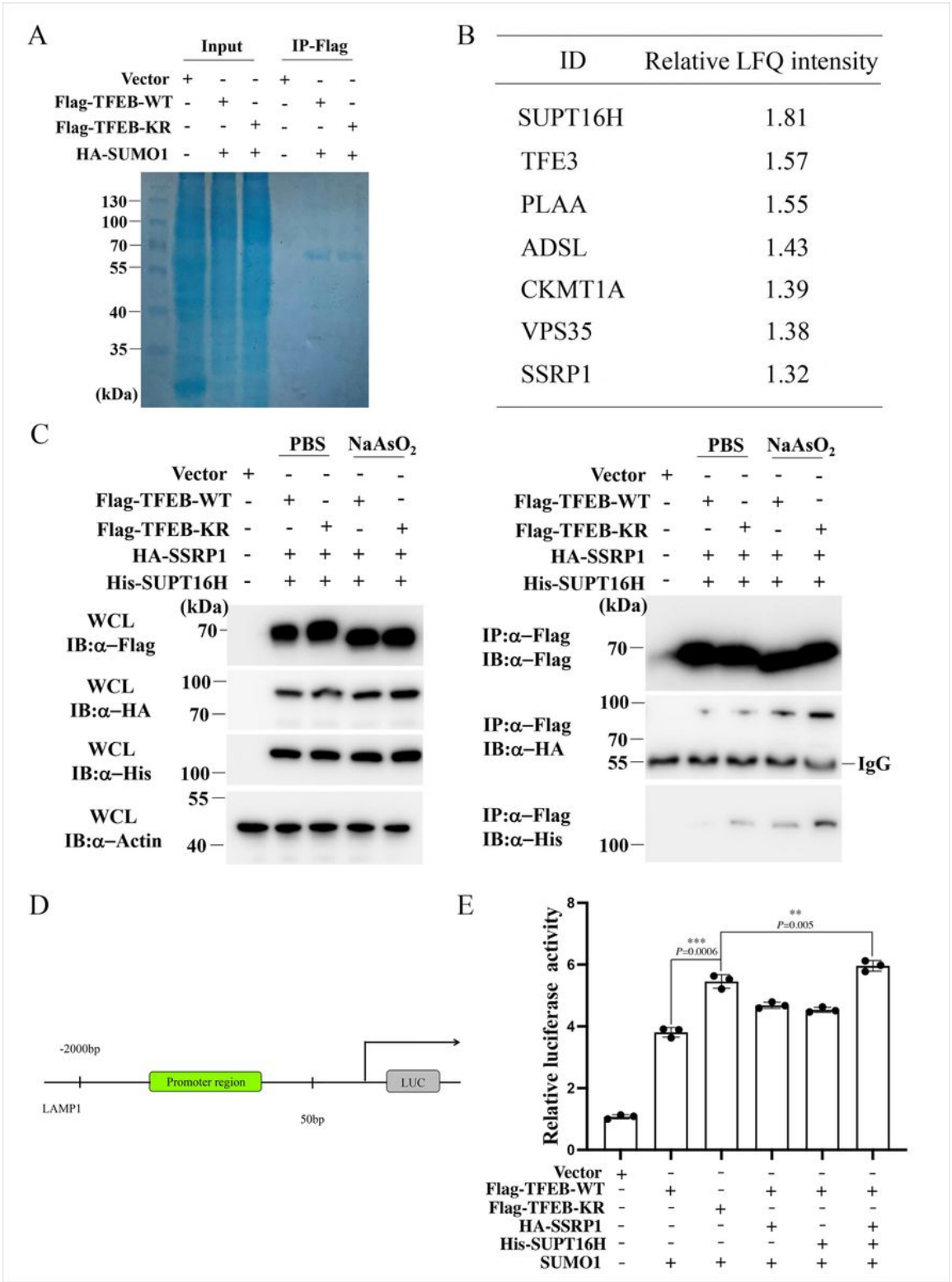

Figure 6

TFEB SUMOylation inhibited the binding between TFEB and FACT complex to attenuate TFEB transcriptional activity.

A: Identification of TFEB related proteins enriched by immunoprecipitation (IP:Flag) using Coomassie brilliant blue staining.

B: Through mass spectrometry analysis, TFEB SUMOylation can affect its interaction with the FACT complex.

C: TFEB SUMOylation is critical for its interaction with FACT complex. 293T cells were transfected with the indicated plasmids, and after 24 hours of transfection, $NaAsO_2$ (250μM) was used to stimulate the cells for 2 hours. Finally, the cells were immunoprecipitated with anti-Flag beads. The precipitated proteins or lysates were immunoblotted with anti-Flag / anti-His or anti-HA antibodies.

D: Schematic diagram of constructing a reporter gene plasmid containing the LAMP1 promoter sequence.

E: The FACT complex can rescue the inhibitory effect of TFEB SUMOylation on its transcriptional activity during OxLDL stimulation. RAW264.7 cells were transfected with indicated plasmids and after 24 hours of transfection, OxLDL (50mg/ml) was used to stimulate the cells for 8 hours. Finally, the activity of the corresponding promoter was checked by report gene assay; n=3.

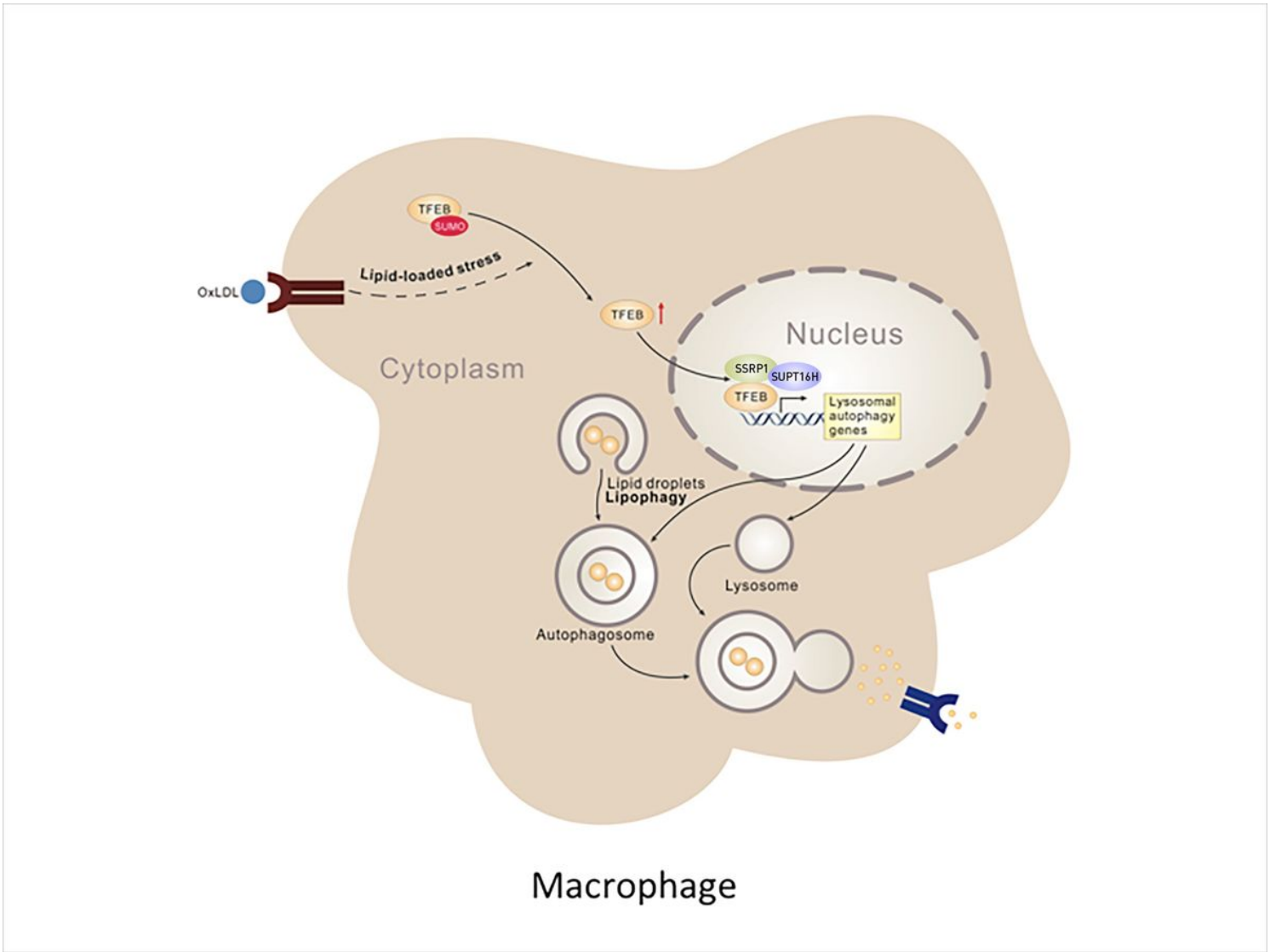

Figure 7

Model depicting the role of TFEB SUMOylation in macrophage foam cells formation.

Under OxLDL stimulation, TFEB would undergo deSUMOylation and deSUMOylation of TFEB has stronger transcriptional activity and promotes lipid degradation by enhancing lysosomal activity, thereby ultimately inhibiting the formation of macrophage foam cells.

Supplementary Files

This is a list of supplementary files associated with this preprint. Click to download.

- Supplementarydata1.tif
- Supplementarydata2.tif
- Supplementarydata3.tif